Performance characteristic and field distribution of a squirrel cage induction motor using finite element analysis

M.M.M. Sedky
Electrical Engg., Dept., Faculty of Engg., Alexandria University, Alexandria Egypt
Email: m_mos2004@yahoo.co.uk

This paper presents the analysis of the induction motor and its behavior during transient condition. Field distribution as well as eddy current distribution in the rotor bars are analyzed. Finite Element Analysis (FEA) was utilized in analyzing the motor characteristic during transient and steady state conditions. The designed geometric dimension of induction motor is modeled in the finite element domain. In the circuit domain, stator windings are distributed in star connection. Coupled electric circuit connects the magnetic circuit with the electrical circuit. Rotor bars are connected in parallel. The rotor motion is included in this model to get the real time simulation results. The transient performance is found at starting with no load, and at different speeds. Simulation results for 2 poles, 3 phase squirrel cage induction motor is presented.

هذا البحث يعرض كيفية و فائدة استخدام حزمة برنامج التحليل بالعناصر المحددة فى كيفية تحليل اداء محرك الحث الذاتى ثلاثى الاوجه. التحليل باستخدام حزمة البرنامج تضمن الحالة الديناميكية للمحرك فى حالة بدء التشغيل والحالة المستقرة. يستفاد ايضا من هذه الحزمة البرمجية بامكانية دراسة توزيع خطوط الفيض المغناطيسى فى العضو الثابت، العضو الدوار، وايضا فى الفراغ بينهما. فى الحيز الكهربى، العضو الثابت مثل بثلاث دوائر كهربية متصلة على شكل نجمة وايضا قضبان العضو الدوار مثلت على هيئة مصادر جهد متصلة على التوازى. يتم الاتصال بين الدوائر الكهربية والمغناطيسية من خلال حزمة البرنامج لتفعيل وتحليل اداء المحرك فى حالات مختلفة من التشغيل

Keywords: Induction motor, Finite element analysis

1. Introduction

Three phase induction motors are extensively used in industries. The performance of the motor during transient periods is difficult to analyze under real time operating condition. Hence simulation methods are used for prediction of transient performance of the induction motor.

Mathematical simulation is not accurate when dealing with the non linear BH curve. On the other hand, FE model takes into account the nonlinearity of the BH curve of the materials. The Finite Element Analysis (FEA), which is a computer based numerical technique, is used for calculating the machine's parameters and design the motor correctly [1-2]. Various parameters of the induction motor, such as Magnetic Vector Potential (MVP), flux density, flux linkage, torque, induced emf, induced eddy current in the rotor bars, and phase current can also be determined [3-5].

2. Induction motor model

Induction motor geometry is designed first using RMxprt package, which has different geometry of stator and rotor slots. There are different stators winding patterns. After designing the geometry of the induction motor by RMxprt, FEA software package solves the electromagnetic field equations, electric circuit equations, and equation of motion. Induction motor geometry can be deigned using Maxwell projects of FEA. The model is created by using version 3.0 of RMxprt and version 10.0 of Maxwell FEA software.

Table 1 lists the parameters of the 2 pole, 3 phases, 380 v, Y, 95 hp induction motor.

2.1. Stator slot data

Fig. 1 shows the stator slot shape, while its dimensions are shown in table 2.

Table1
Motor parameters

Parameter	Value
Number of pole	2
Number of stator slots	36
Number of rotor slots	28
Stator outer diameter (inches)	10.125
Rotor outer diameter (inches)	5.525
Shaft diameter (inches)	1.875
Air gap (inches)	0.046
Stack length (inches)	9.5
Stator and rotor material	steel type (D23)

Table 2
Stator and rotor slots dimensions

Stator	Value stator	Rotor	Value rotor
Hs0	0.0555	Hr0	0.0215
Hs1	0.065	Hr01	0
Hs2	0.698	Hr1	0.01
Bs0	0.16	Hr2	0.44
Bs1	0.309	Br0	0.01
Bs2	0.432	Br1	0.3
		Br2	0.2

2.2. Rotor slot data

Fig. 2 shows the rotor slot shape, while its dimensions are given in table 2. The geometry of the model is modeled in FEA, as shown in fig. 3.

Material properties are assigned to the motor components, where stator windings and rotor bars are assigned as copper material.

Stator and rotor body are assigned as steel with the BH curve as shown in fig 4.

The Shaft is assigned as steel with constant permeability, the air gap between the rotor and stator is assigned as an air, the region outside the stator is assigned as a vacuum. In transient solver we need to build a band region to envelop all the rotational parts (rotor, bars, and shaft).

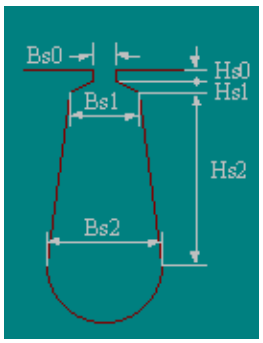

Fig. 1. Stator slot shape.

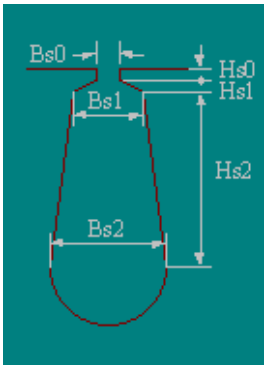

Fig. 2. Rotor slot shape.

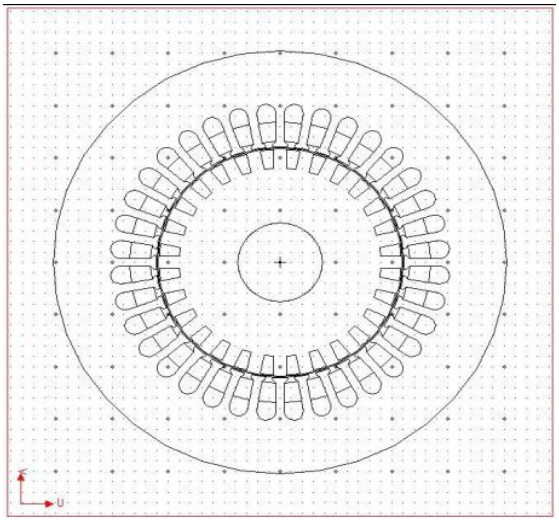

Fig. 3. FEA geometry of induction motor.

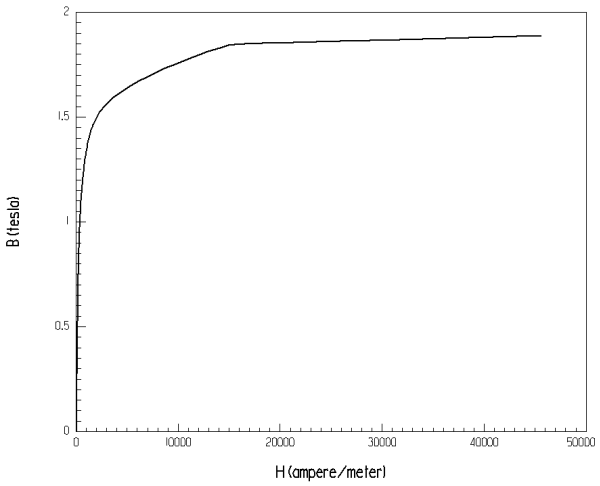

Fig. 4. BH curve of the stator and rotor material.

Each phase of the stator three phase sources is divided into two groups, for go and return current. Phase A has PHAgo and PHAret, phase B has PHBgo, and PHBret, Phase C has PHCgo and PHCret.

Rotor bars are all connected as one group. The whole model is discretized into small elements, where the more elements are used, the more accurate solution results. Fig. 5 shows the mesh model of the induction motor.

2.3. Circuit modeling

All stator and rotor conductor areas are represented in the circuit domain of FEA.

Stator windings are assigned stranded conductors, with resistances and inductances added to each phase. In the circuit schematic diagram, stator windings are assigned star connection with three phase supply applied to them.

Fig. 6 shows the three phase winding of the stator winding. Rotors bars are considered as parallel winding, (for the squirrel cage case).

3. Maxwell's equations

The transient solver of the FEA allows solving and analyzing the magnetic fields, energy, force, power, power loss, speed, and flux of the model at various time steps of a solution over a specified period of time. It allows a non sinusoidal current or voltage excitation, as well as rotational or translational motion. The transient solver of the FEA assumes the following conditions about the problem:

1- If motion occurs in the model, no motion occurs outside the band object.

2- Only one type of motion (translational or rotational) occurs in the model.

3- More than one object can be assigned identical motion within the band object.

The time-dependent magnetic field is expressed in eq. (1)

$$\nabla \times \upsilon \nabla \times A =$$

$$J_s - \sigma \frac{\partial A}{\partial t} - \sigma \nabla v + \nabla \times H_c + \sigma v \times \nabla \times A. \qquad (1)$$

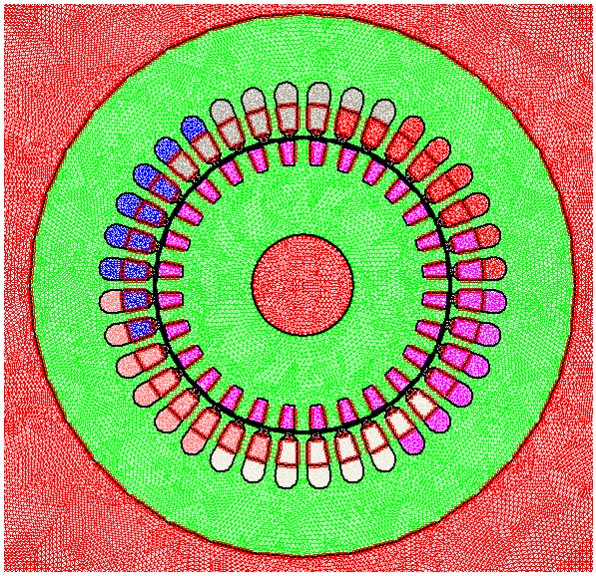

Fig. 5 Mesh distribution of the FEA model.

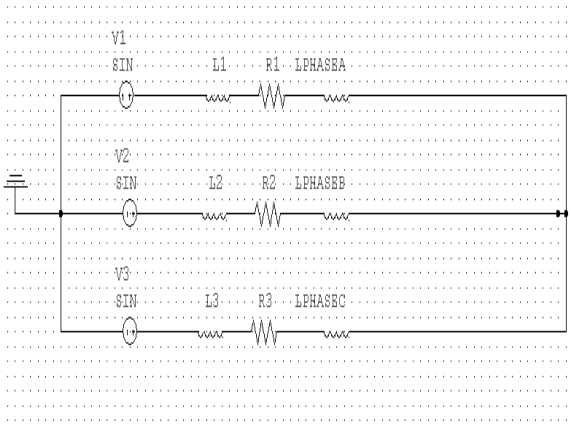

Fig. 6. The external electric circuit of the stator circuit.

Where,

H_C is the coercivity of the permanent magnet, (If found in the model),

v is the velocity of the moving parts,

A is the magnetic vector potential, and

J_s is the source current density.

The transient solver applies a reference frame that is fixed with respect to the components in the model by setting the velocity, υ, equal to zero. Because the moving components have now been fixed to their own coordinate system, the partial time derivative becomes in the total time derivative of A. Thus, the motion equation becomes eq. (2):

$$\nabla \times \upsilon \nabla \times A =$$

$$J_s - \sigma \frac{dA}{dt} - \sigma \nabla v + \nabla \times H_c . \quad (2)$$

The induction motor has two types of current source: stranded and solid. Stator winding are assigned as a stranded current source, where stranded conductors lack eddy current behavior and are considered to be filaments too thin to model in a practical finite element grid. Because of this, the transient solver assumes that their contribution to the current density is averaged over the area of problem region. The current density is based on eq. (3).

$$\nabla \times \upsilon \nabla \times A = J_s . \quad (3)$$

Rotor bars are assigned parallel solid conductor where solid conductor is large enough to model with finite element. The skin effect depends not only on the frequency of the system, but on the location of nearby conductors. Based on Ampere's law, the total current density, J_t, in the system is given by eqs. (4 – 6).

$$J_t = J_e + J_s \ . \quad (4)$$

Where:

$$J_t = -\sigma \frac{\partial A}{\partial t} - \sigma \nabla v . \quad (5)$$

Which reduces to

$$J_t = -\sigma \frac{\partial A}{\partial t} + \frac{\sigma}{l} V_b \ . \quad (6)$$

Where,

V_b is the voltage difference across the conductors end points,

J_e is the eddy current density, and

Js is the source current density.

Rotational motion

The transient motion simulator generates rotational motion based on the following motion eq. (7).

$$J\beta + D\omega = T_{comp} + T_{load} . \quad (7)$$

Where:

J is the inertial force, in kg.m^2

T is the torque, in N.m

ω is the angular speed, in rad/sec

β is the angular acceleration, in rad/sec^2, and

D is the damping factor, in N.m.s.

4. Induction motor starting analysis

The system is analyzed in the transient solver, with no load condition. The winding of phase A, B and C of the stator have equal number of turns. The stator circuit is excited by a three phase supply, of 380/220 v, rms value. The voltage eqs. (8-10) are as follows:

$$V_a = R_a I_a + p\lambda_a . \quad (8)$$

$$V_b = R_b I_b + p\lambda_b . \quad (9)$$

$$V_c = R_c I_c + p\lambda_c . \quad (10)$$

Time step is playing a vital role in the analysis, because the smaller time step, the more accurate the results. Time step is chosen here to be 1/20 of the period cycle of the input power supply.

Fig. 7 shows the three phase applied voltage for the stator circuit. The speed variation of the motor with time is shown in fig. 8, where the synchronous (no load) speed, N_s, for 2 pole, 50 Hz, 3 phase machine is 3000 rpm.

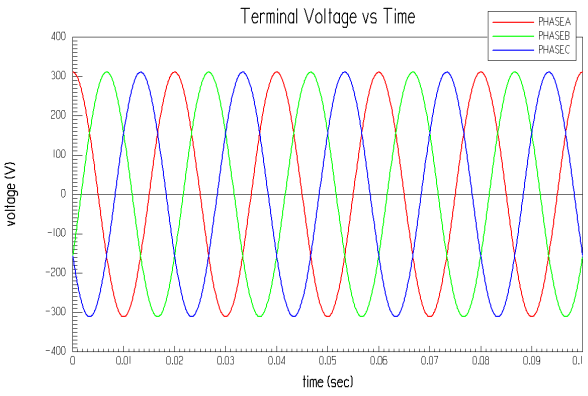

Fig. 7. The three phase input voltage.

From fig. 8, the speed is reached to the synchronous speed and maintained constant before 0.15 sec, and the same in fig 9 for the 3 phase currents; the starting current is very high then damped to the no load current before t = 0.15 sec.

Fig. 10 shows the back emf generated in the three phase windings due to the differentiate of the flux linakge which is shown in fig. 11.

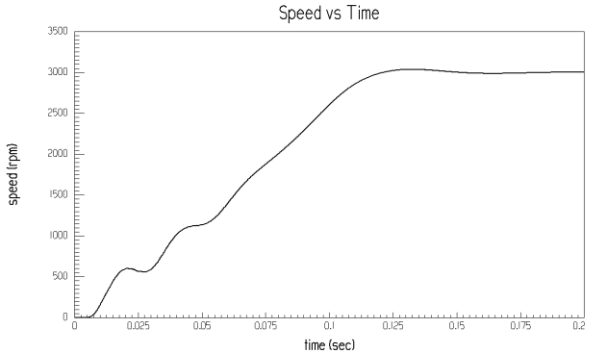

Fig. 8. Induction motor speed (rpm).

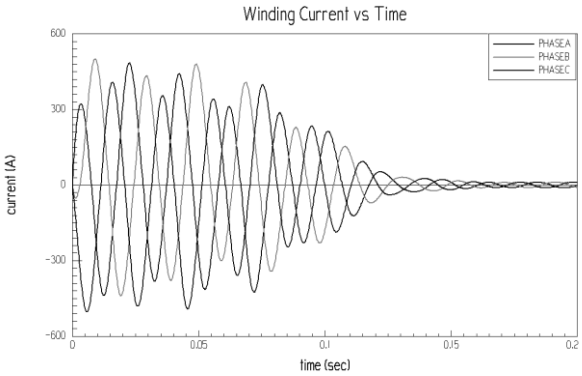

Fig. 9. The 3 phase stator currents.

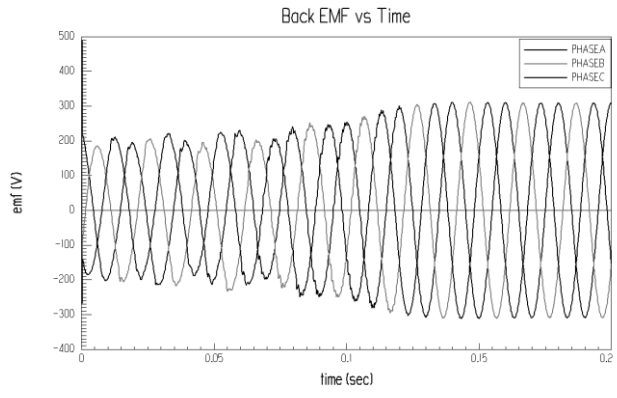

Fig.10. The three phase back emf.

Torque pattern is shown in fig. 12, where the developed torque ends to zero at synchronous speed.

5. Magnetic analysis

Transient solver of FEA gives the ability to study the magnetic pattern of the machine at different time steps.

Flux distribution along a complete one cycle at different times is shown in fig. 13, a-e, where the FEA gives a clear idea about the concept of the rotating magnetic field in the AC 3 phase machine.

The scalar quantity of the magnetic flux distribution along the inner contour is shown in fig. 14, where the contour is passing along the middles of the rotor bars. The magnetic flux is sinusoidally distributed along the rotor bars as shown in fig. 15. Rotor's current density along the same contour is shown in fig. 14, where the induced current is proportional to the magnitude of the air gap flux and its direction as well.

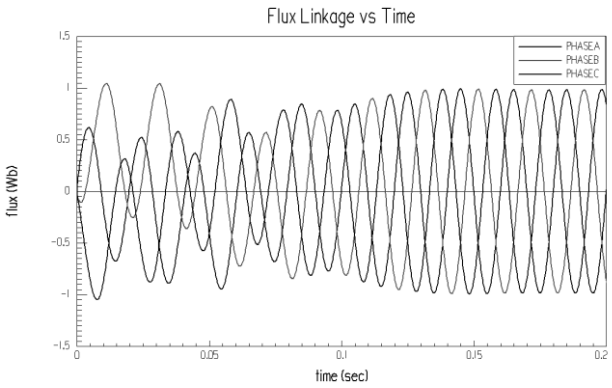

Fig. 11. The three flux linkage.

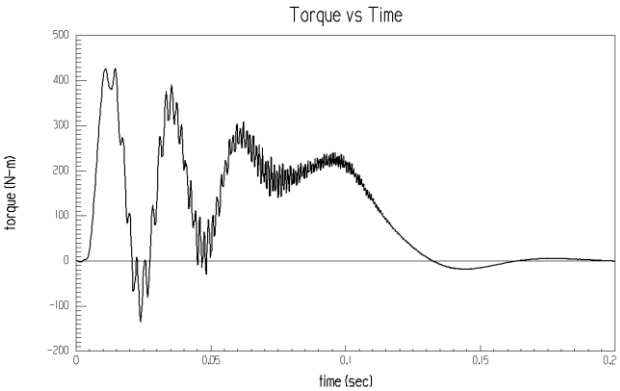

Fig.12. Electromagnetic torque.

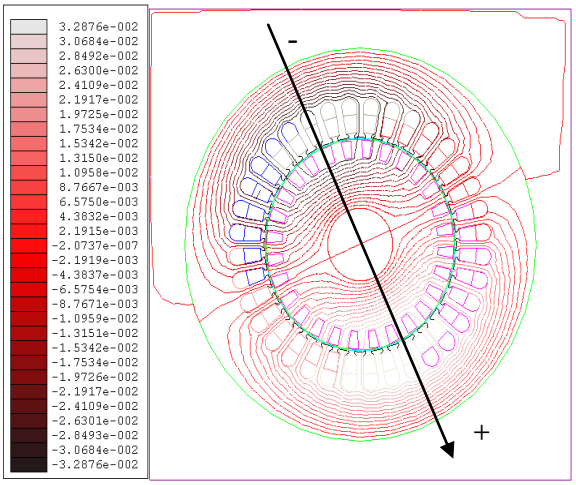

Fig. 13-a. Magnetic flux distribution at t = 0.2 sec.

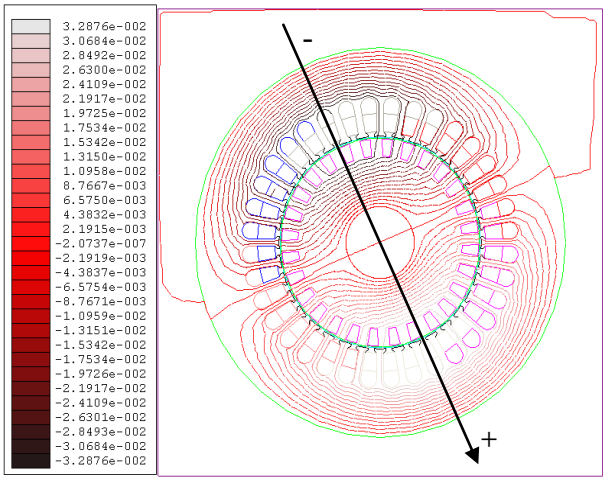

Fig. 13-b. Magnetic flux distribution at t = 0.2 sec.

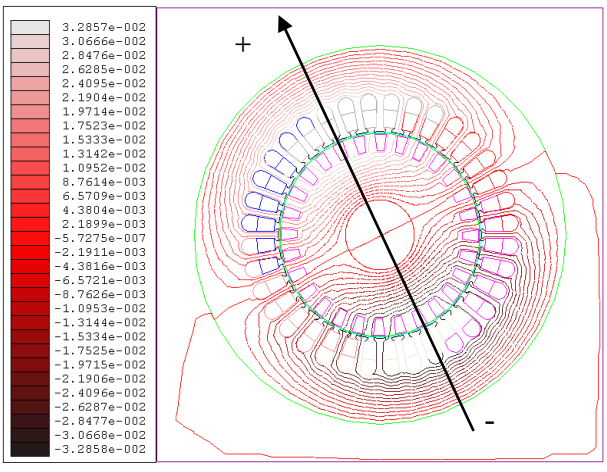

Fig. 13-c. Magnetic flux distribution at t = 0.21 sec.

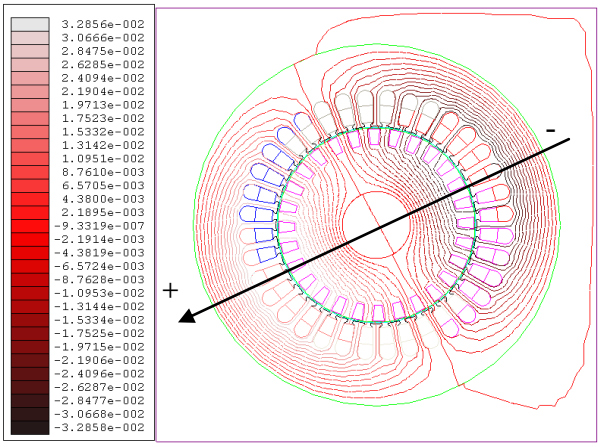

Fig. 13-d. Magnetic flux distribution at t= 0.215 sec.

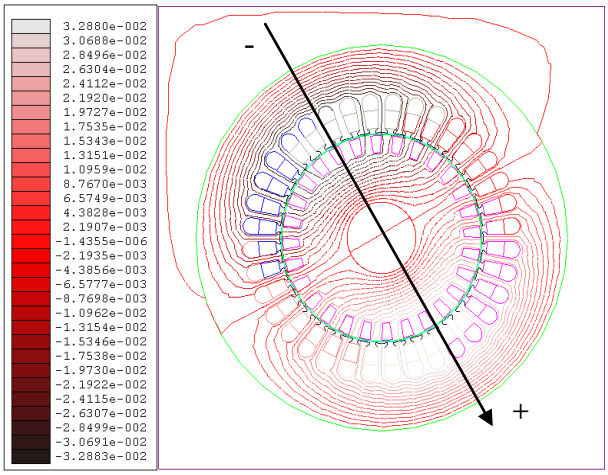

Fig. 13-e. Magnetic flux distribution at t= 0.22 sec.

The rotors current density is sinusoidally distributed along the bars and the summation of the entire induced current equal zero. Current distribution along every bar is due to the skin effect, where it is concentrated around the bars edges and less in the middle.

Stator current source is considered to be stranded conductors, so the current is uniformly distributed along all the bars according to the equation of three phase current in time domain. At that time phase A has positive maximum while B and C have negative half the maximum values as shown in fig. 18. This is what is shown here along the chosen contour in the middle of stators bars, fig. 17. The current distribution of the stator is drawn at a time step located in the steady state region, where all the currents have the

same steady state equation, while not taking in the transient condition because in this interval the current has non defined formula to check the response.

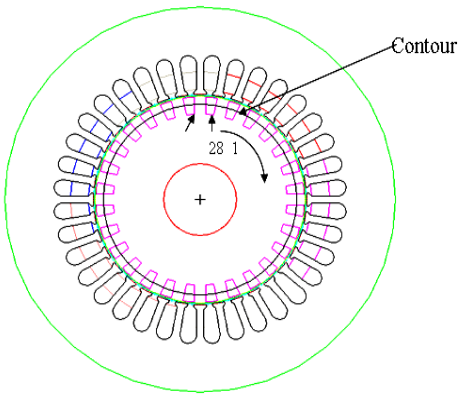

Fig. 14. Rotor contour

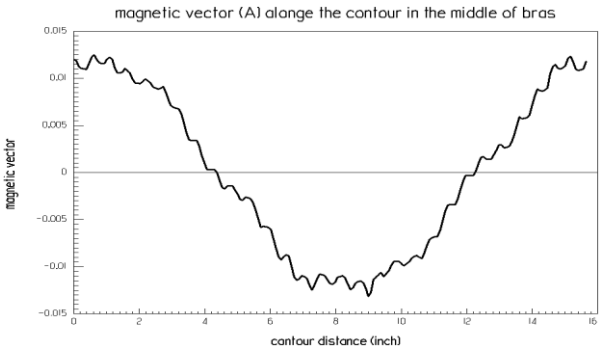

Fig.15. Magnetic field quantity under the middle of the rotor bars.

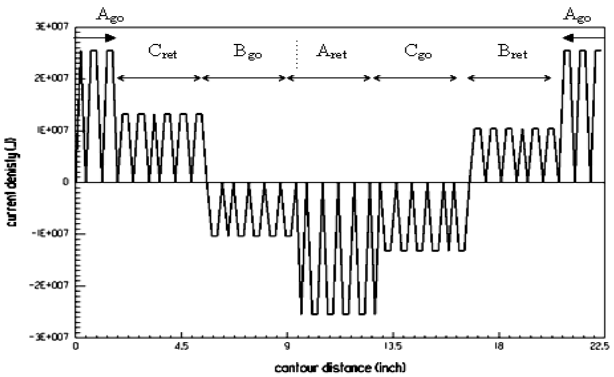

Fig. 16. Current density distribution along the bars, in the middle.

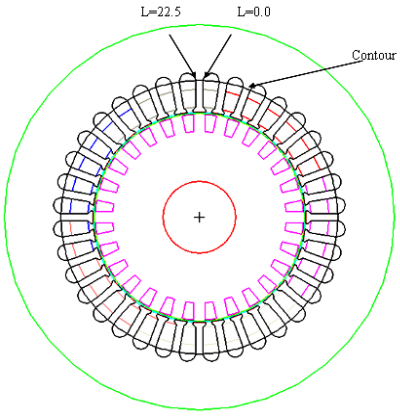

Fig. 17. Stator contour.

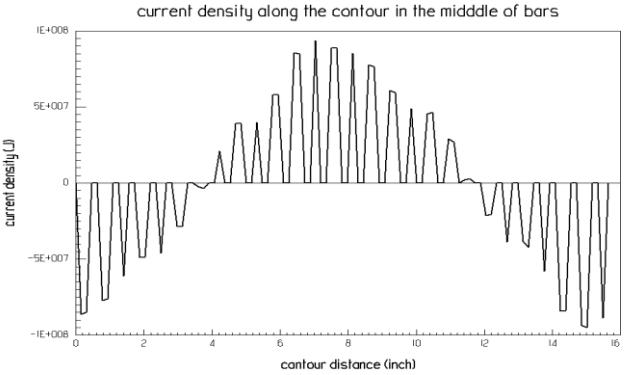

Fig. 18. Stator currents distribution along the contour.

6. Transient analysis at load condition

Transient solver of FEA has the facility of modeling the induction motor under different load conditions.

In motion setup filed, moment of inertia is added, and rotor speed is defined in rpm. Figs. 19 and 20 show the 3 phase current transient at different slips, 0.01 and 0.1, where the corresponding torque for the two values are in figs. 21 and 22.

7. Conclusions

Induction motor modeling using the coupled electric circuit with two-dimensional Finite Element Electromagnetic (FEA) analysis is explained. Transient performance is tested at no load, and at load condition. The torque pattern is verified using FEA. Flux behavior and its distribution are analyzed by FEA. FEA helps to analysis any abnormal condition.

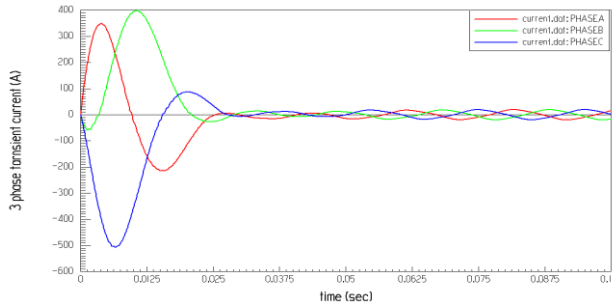

Fig. 19. Transient current at s = 0.01.

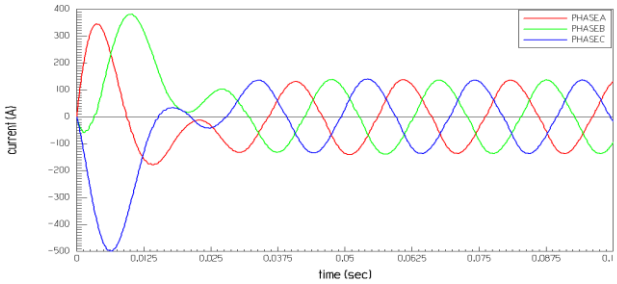

Fig. 20. Transient current at s = 0.1.

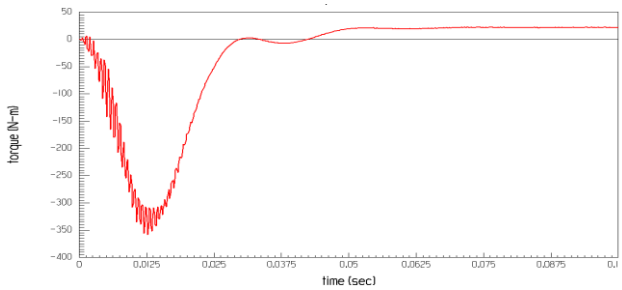

Fig. 21. Developed torque at s = 0.01.

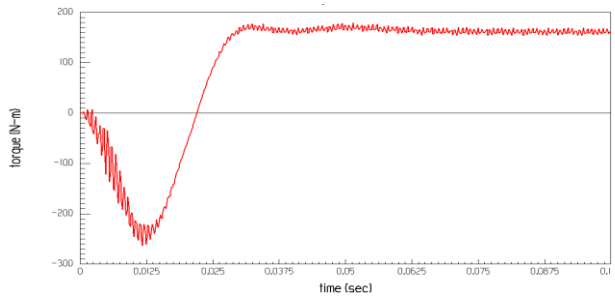

Fig. 22. Developed torque at s = 0.1.

References

[1] S. Williamson, L.H. Lim and A.C. Smith, "Transient Analysis of Cage Induction Motor Using Finite Elements", IEEE Transaction on Magnetic, Vol. 26 (2), March, pp. 941-994 (1990).

[2] Bhoj Raj Singla, Sanjay Marwaha and Anupma Marwaha, "Design and Transient Analysis of Cage Induction Motor Using Finite Element Methods", International Conference on Power Electronics, Drives and Energy Conversion Systems, PEDES, 12-15, Dec., pp. 1-5 (2006).

[3] Tan H. Palm, Philippe F. Wendling, Sheppard J. Salon and Harun Acikgoz, "Transient Finite Element Analysis of Induction Motor with External Circuit Connections and Electromechanical Coupling", IEEE Transaction on Energy Conversion, Vol. 14 (4), pp. 1407-1412 (1999).

[4] Stephen Williamson, Lian Hoon Lim and Michael J. Robinson, "Finite Element Models for Cage Induction Motor Analysis", IEEE Transaction on Industry Applications. Vol. 26 (6), November. pp. 1007-1016 (1990).

[5] S. Williamson and M.J. Robison, "Calculation of Cage Induction Motor Equivalent Circuit Parameters Using Finite Elements", IEEE Proceeding- B. Vol. 138 (5), pp. 264-276 (1991).

[6] P.C. Sen., Principle of Electric Machines Power Electronics, John Willy and Sons, New York.

[7] Li Weili, Xie Ying, Shen Jiafeng and Luo Yingli, "Finite Element Analysis of Field Distribution and Characteristic Performance of Squirrel Cage Induction Motor with Broken Bars", IEEE Transactions on Magnetic, Vol. 43 (4), pp. 1537-1540 (2007).

Received July 26, 2008
Accepted March 30, 2009